

# Towards data analysis with diagrammatics

**Tobias Kühn**

Institut de la Vision, Sorbonne Université, CNRS, INSERM, 17 rue Moreau,  
75012 Paris, France

**Abstract.** Systems with many interacting stochastic constituents are fully characterized by their free energy. Computing this quantity is therefore the objective of various approaches, notably perturbative expansions, which are applied in problems ranging from high-dimensional statistics to complex systems. However, a lot of these techniques are complicated to apply in practice because they lack a sufficient organization of the terms of the perturbative series. In this manuscript, we tackle this problem by using Feynman diagrams, extending a framework introduced earlier to the case of free energies at fixed variances. These diagrammatics do not require the theory to expand around to be Gaussian, which allows its application to the free energy of a spin system studied to derive message-passing algorithms by Maillard et al. 2019. We complete their perturbative derivation of the free energy in the thermodynamic limit. Furthermore, we derive resummations to estimate the entropies of poorly sampled systems requiring only limited statistics and we revisit earlier approaches to compute the free energy of the Ising model, revealing new insights due to the extension of our framework to the free energy at fixed variances. We expect our approach to be useful also for future applications, notably for problems of high-dimensional statistics, like matrix factorization, and the study of complex networks.

## 1. Introduction

A lot of interesting and challenging problems in physics are composed of multiple complicated, but well characterized components, who interact in a pairwise fashion. This concerns, for example, spin systems (Ising, Potts, XY, Heisenberg, p-spin,...), in which the single components are connected by pairwise interactions, or simple liquids, which consist of particles that interact in a pairwise way and would otherwise form an ideal gas [5].

When modelling complex systems, we often know the cumulants of the single elements constituting the ensemble and the covariances between them, but not more. There are plenty of examples for data of this kind, for example electrophysiological recordings from neuronal populations, measurements of the densities of animals inside a flock or a herd or genetic data. In none of these cases, the underlying microscopic theory is known - or if it is, it is not practically feasible to use it for predictions. Therefore, effective models, borrowed from the microscopic description of spins, are in use there. A popular and successful strategy in these examples is to employ the reasoning of maximum entropy: given some statistical measures, like, for example, then mean of a variable, one chooses among all probability distributions reproducing them that one with the highest entropy [7]. For binary variables with given means and covariances, the resulting probability distribution is that of an Ising spin glass, which is therefore a widespread tool in the modeling of complex systems.

While with the first scenario of an a-priori given theoretical model with known parameters we are invoking a forward problem, we address an inverse problem in the second case: finding the parameters of a model given some observations. In both scenarios, computing the free energies of the respective systems means basically “solving” the system: in the forward case, the free energy allows to obtain all possible moments by taking derivatives, in the inverse case, the same is true for the parameters of the system. In the latter case, furthermore, the free energy is equal to the maximum entropy, which is often interesting on its own.

In this study, we tackle the problem of computing the free energy at fixed means and variances for both cases, that is given interactions and given covariances. For the forward problem, we will expand in small couplings, for the inverse problem in small covariances.

While these kind of expansions are not a novel concept, but can be traced back at least to the seminal work of Plefka [18] from 1982, on which follow-up work has built ever since [2, 3, 6, 14, 17, 19], there are still problems that cannot be solved with the techniques developed in these studies. Indeed, in a quite recent publication, Maillard et al. [12] address the problem of deriving the free energy of p-spins coupled by a symmetric rotationally invariant matrix. The use of the formalism of [3] allows them to conjecture its form in the thermodynamic limit, but not to give the complete proof.

In this manuscript, we pick up these lines of thought, however, developing them in terms of Feynman diagrams. As opposed to most other diagrammatic frameworks, we will not assume the theory to expand about to be Gaussian. By extending the applicability of Feynman diagrammatics, we leverage the strength of this concept - that it simplifies and structures computations - to expansions around non-Gaussian theories. This allows us to complete the proof of Maillard et al, in section 3.1. Furthermore, we show, in section 3.2, how to use our framework in a inverse-problem setting to derive approximations for the entropy of complex systems [10] and we discuss how extending the Legendre transform to encompass the variance helps to understand

earlier results on perturbation theory for the Ising model [2, 9, 20, 21] (section 3.3).

We derive the technical results on Feynman diagrammatics in section §2 - for the expansion in small couplings in section 2.1 and for small covariances in section 2.2 -, using and extending techniques from our earlier works [9, 11]. In the discussion, we give an outlook on possible applications of our approach, including the derivation of message-passing algorithms for matrix denoising and factorization [13], the study of higher-order correlations in complex systems and further insights into the diagrammatics of the Ising model.

## 2. Methods

Consider a (Helmholtz) free energy of the form

$$W[\mathbf{j}, \mathbf{k}] = \ln \left( \sum_{\psi} e^{\frac{\beta}{2} \sum_{i \neq j} K_{ij} \psi_i \psi_j + \sum_i (j_i \psi_i + k_i^2 \psi_i^2)} \right), \quad (1)$$

where  $\psi$  is a discrete index. It could also be continuous, in which case the sum over it would be an integral, an option however that we will not consider in this manuscript.

### 2.1. The Legendre transform with respect to one-point source fields: $\Gamma^K$

Fixing the mean and the variance of the single spins, we obtain the (Gibbs) free energy

$$\Gamma^K[\mathbf{m}, \mathbf{v}] := \sup_{\mathbf{j}, \mathbf{k}} \left[ \sum_i m_i j_i + (v_i + m_i^2) k_i - W[\mathbf{j}, \mathbf{k}, K] \right] \quad (2)$$

as a Legendre transform of equation (1). Differentiating  $\Gamma^K$  with respect to its arguments, we obtain the equations of state

$$\frac{\partial \Gamma^K}{\partial m_i} = j_i + 2m_i k_i \quad (3)$$

$$\frac{\partial \Gamma^K}{\partial v_i} = k_i \quad (4)$$

*2.1.1. Derivation of the perturbative expansion for  $\Gamma^K$*  Analogous to [9, 11], we will rewrite equation (2) in order to derive an expansion of  $\Gamma^K$  in the couplings  $K_{ij}$ , in which we structurally take into account its definition as a Legendre transform. Necessarily, considerable parts of what follows are paraphrases of [9, 11], which we include to make this manuscript readable on its own. To prepare the implementation of this expansion, we derive an expression for  $\Gamma^K$  without explicit reference to the Legendre transform as a supremum. We use the definition of  $\Gamma^K$ , equation (2), together with the equations of state, equation (3) and equation (4), through which we express  $\mathbf{j}$  and  $\mathbf{k}$ , to arrive at

$$\begin{aligned} & \exp \left( -H[\psi] + \mathbf{j}^T \psi + \frac{1}{2} \psi^T K \psi \right) = \exp(W[\mathbf{j}, K]) \\ & = \exp \left( \mathbf{m}^T \mathbf{j} + (\mathbf{v} + \mathbf{m}^2)^T \mathbf{k} - \Gamma^K[\phi, \Delta] \right) \\ & = \exp \left( \mathbf{m}^T \left( \frac{\partial \Gamma^K}{\partial \mathbf{m}} - 2 \frac{\partial \Gamma^K}{\partial \mathbf{v}} \odot \mathbf{m} \right) + (\mathbf{v} + \mathbf{m}^2)^T \frac{\partial \Gamma^K}{\partial \mathbf{v}} - \Gamma^K[\mathbf{m}, \mathbf{v}] \right), \end{aligned}$$

where by  $\odot$  we denote element-wise multiplication. We finally isolate  $\Gamma^K$  and replace the field  $\boldsymbol{\psi}$  by its expression as a derivative with respect to  $\boldsymbol{j}$ . This leads to

$$\begin{aligned} & \exp(-\Gamma^K[\mathbf{m}, \mathbf{v}]) \\ &= \sum_{\boldsymbol{\psi}} \exp\left(-H[\boldsymbol{\psi}] + (\boldsymbol{\psi} - \mathbf{m})^T \left(\frac{\partial \Gamma^K}{\partial \mathbf{m}} - 2\frac{\partial \Gamma^K}{\partial \mathbf{v}} \odot \mathbf{m}\right) + \frac{\partial \Gamma^K}{\partial \mathbf{v}} [(\boldsymbol{\psi}^2 - \mathbf{m}^2) - \mathbf{v}]\right) \end{aligned} \quad (5)$$

At this stage, no approximation has been made, and equation (5) is fully exact. Next, we will use this expression to set up the small-coupling expansion for the quantity  $\Gamma^K$ .

We separate the Hamiltonian and the free energies into a solvable and a perturbing part, according to

$$\Gamma^K = \Gamma_0^K + \Gamma_v^K$$

and analogous for  $H$  and  $W$ . Plugging this decomposition into equation (5), isolating  $-\Gamma_v^K$  on the left-hand side, reuniting the  $\Gamma_0^K$  with its derivatives to re-obtain  $W_0$ , we get

$$\begin{aligned} & \exp(-\Gamma_v^K[\mathbf{m}, \mathbf{v}]) \\ &= e^{-W_0[\mathbf{j}_0, \mathbf{k}_0]} e^{-H_v[\frac{\partial}{\partial \mathbf{j}}] + \left(\frac{\partial \Gamma_0^K}{\partial \mathbf{m}}\right)^T \left(\frac{\partial}{\partial \mathbf{j}} - \mathbf{m}\right) + \frac{\partial \Gamma_0^K}{\partial \mathbf{v}} [(\frac{\partial}{\partial \mathbf{j}} - \mathbf{m})^2 - \mathbf{v}]} e^{W_0[\mathbf{j}, \mathbf{k}_0]} \Bigg|_{\mathbf{j}=\mathbf{j}_0, \mathbf{k}=\mathbf{k}_0}, \end{aligned} \quad (6)$$

where

$$\mathbf{j}_0 = \frac{\partial \Gamma_0^K}{\partial \mathbf{m}} - 2\frac{\partial \Gamma_0^K}{\partial \mathbf{v}} \odot \mathbf{m}$$

$$\mathbf{k}_0 = \frac{\partial \Gamma_0^K}{\partial \mathbf{v}},$$

in words, we choose the source fields such that the unperturbed theory reproduces the measured statistics. As in [9, 11], we define a differential operator for convenience, as

$$A_J \left(\frac{\partial}{\partial \mathbf{j}}\right) := -H_v \left[\frac{\partial}{\partial \mathbf{j}}\right] \quad (7)$$

$$+ \left(\frac{\partial \Gamma_0^K}{\partial \mathbf{m}}\right)^T \left(\frac{\partial}{\partial \mathbf{j}} - \mathbf{m}\right) \quad (8)$$

$$+ \left(\frac{\partial \Gamma_0^K}{\partial \mathbf{v}}\right)^T \left[\left(\frac{\partial}{\partial \mathbf{j}} - \mathbf{m}\right)^2 - \mathbf{v}\right] \quad (9)$$

and write

$$\exp(-\Gamma_v^K[\mathbf{m}, \mathbf{v}]) = e^{-W_0[\mathbf{j}_0, \mathbf{k}_0]} \lim_{L \rightarrow \infty} \left(1 + \frac{1}{L} A_J \left(\frac{\partial}{\partial \mathbf{j}}\right)\right)^L e^{W_0[\mathbf{j}, \mathbf{k}_0]} \Bigg|_{\mathbf{j}=\mathbf{j}_0, \mathbf{k}=\mathbf{k}_0} \quad (10)$$

so that we can compute  $\Gamma_v^K[\mathbf{m}, \mathbf{v}]$  as a series expansion by evaluating the perturbing terms order by order in the interaction  $K$ . To organize the expansion in  $K$ , we define [9, 11]

$$e^{g_{l,L}[\mathbf{j}, \mathbf{k}]} = \left(1 + \frac{1}{L} A_J \left(\frac{\partial}{\partial \mathbf{j}}\right)\right)^l e^{W_0[\mathbf{j}, \mathbf{k}]}.$$

We read off from equation (10) that

$$-\Gamma_v^K[\mathbf{m}, \mathbf{v}] = -W_0[\mathbf{j}_0, \mathbf{k}_0] + \lim_{L \rightarrow \infty} g_{L,L}[\mathbf{j}_0, \mathbf{k}_0] =: -W_0[\mathbf{j}_0, \mathbf{k}_0] + \lim_{L \rightarrow \infty} g[\mathbf{j}_0, \mathbf{k}_0].$$

By definition, we have

$$e^{g_{l+1,L}[\mathbf{j},\mathbf{k}]} = \left(1 + \frac{1}{L} A_J \left(\frac{\partial}{\partial \mathbf{j}}\right)\right) e^{g_{l,L}[\mathbf{j},\mathbf{k}]},$$

so that we obtain the recursion relation

$$\begin{aligned} & g_{l+1,L}[\mathbf{j},\mathbf{k}] - g_{l,L}[\mathbf{j},\mathbf{k}] \\ &= -\frac{1}{L} e^{-g_{l+1,L}[\mathbf{j},\mathbf{k}]} H_V \left[\frac{\partial}{\partial \mathbf{j}}\right] e^{g_{l+1,L}[\mathbf{j},\mathbf{k}]} \\ & \quad + \frac{1}{L} e^{-g_{l+1,L}[\mathbf{j},\mathbf{k}]} \left(\frac{\partial \Gamma^K}{\partial \mathbf{m}}\right)^T \left(\frac{\partial}{\partial \mathbf{j}} - \mathbf{m}\right) e^{g_{l+1,L}[\mathbf{j},\mathbf{k}]} \\ & \quad + \frac{1}{L} e^{-g_{l+1,L}[\mathbf{j},\mathbf{k}]} \left(\frac{\partial \Gamma^K}{\partial \mathbf{v}}\right)^T \left[\left(\frac{\partial}{\partial \mathbf{j}} - \mathbf{m}\right)^2 - \mathbf{v}\right] e^{g_{l+1,L}[\mathbf{j},\mathbf{k}]} + \mathcal{O}\left(\frac{1}{L^2}\right). \end{aligned}$$

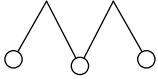
Note that in first order of the interaction, only  $H_V \left[\frac{\partial}{\partial \mathbf{j}}\right]$  contributes, whereas the contributions of the other two parts cancel by construction - as it has to be because of the properties of the Legendre transform. We can therefore construct the small- $K$  expansion of  $\Gamma^K$  order by order, keeping track of all terms denoting them by Feynman diagrams. Their constituting elements are

$$\begin{array}{ccc} \begin{array}{c} i \quad j \\ \delta_{j_i} \delta_{j_j} \delta_{j_k \dots} \end{array} & = \frac{\delta^n W}{\delta j_i \delta j_j \delta j_k \dots}, & \begin{array}{c} i \quad j \\ \dots \\ \dots \end{array} & = \kappa_{i,j,k,\dots}^n, & & = K_{ij}. \end{array} \quad (11)$$

*2.1.2. Diagrammatics of  $\Gamma^K$*  As for the first Legendre transform (with respect to  $\mathbf{j}$  only) the first two orders of  $\Gamma^K$  are given as

$$\Gamma^J[\mathbf{m},\mathbf{v}] = \Gamma_0^J[\mathbf{m},\mathbf{v}] - \begin{array}{c} \diagup \quad \diagdown \\ \circ \quad \circ \end{array} - \begin{array}{c} \diagup \quad \diagdown \\ \diagdown \quad \diagup \\ \circ \quad \circ \end{array} + \dots \quad (12)$$

As shown in [9], the contribution equation (8) to the differential operator  $A \left(\frac{\partial}{\partial \mathbf{j}}\right)$  removes all one-line reducible diagrams - that is, all diagrams from the expansion of  $W$  (that is, all connected diagrams, according to the linked-cluster theorem [9, 24, appendix A.3]) that can be split into two parts by cutting a leg of an interaction (represented by an edge). In second order in  $K$  for example, this means that the diagram



is canceled in the expansion of  $\Gamma^K$ . In the following, we convince ourselves that the effect of equation (9) is analogous and concerns two-particle reducible diagrams. For illustrative purposes, we will start with the fourth order and then generalize.

*2.1.3. Cancellations in fourth order* The lowest-order contribution to equation (9) is given by

$$\frac{\partial \Gamma^J}{\partial v_i} \supseteq - \begin{array}{c} \square \\ \bullet \end{array} = -\frac{\partial}{\partial v_i} \frac{1}{4} \sum_{k \neq j} v_k J_{kj}^2 v_j = -\frac{1}{2} \sum_{j(\neq i)} J_{ij}^2 v_j, \quad (13)$$

where by the broken lines we indicate identical indices from now on. We recall from equation (11) that full nodes indicate cumulants, that is, the cumulant-generating functional evaluated at  $\mathbf{j}_0$  and  $\mathbf{k}_0$ . The additional interaction in equation (13) generates the two types of additional diagrams. First the ones of the “spectacles” topology

$$- \begin{array}{c} J \quad J \\ \diagdown \quad \diagup \\ \circ \quad \circ \\ \diagup \quad \diagdown \\ J \quad J \end{array} + \frac{\partial \Gamma^K}{\partial \mathbf{v}} \begin{array}{c} \bullet \quad J \\ \diagdown \quad \diagup \\ \circ \quad \circ \\ \diagup \quad \diagdown \\ J \quad \bullet \end{array} - \frac{\partial \Gamma^K}{\partial \mathbf{v}} \begin{array}{c} \bullet \quad \bullet \\ \diagdown \quad \diagup \\ \circ \quad \circ \\ \diagup \quad \diagdown \\ \bullet \quad \bullet \end{array} = 0, \quad (14)$$

where we denote cumulants inside  $\frac{\partial \Gamma^K}{\partial \mathbf{v}}$  vertices with full nodes to highlight their origin - they translate into the same expressions as the empty nodes, however. More generally, diagrams composed of multiple rings attached at one point are known as cactus diagram [12, 16, 17]. The spectacles diagrams come about by letting both derivatives associated to the  $\frac{\partial \Gamma^K}{\partial \mathbf{v}}$  vertex act on the same cumulant. The other possibility is to generate two cumulants of order two. This yields

$$- \begin{array}{c} \circ \\ \diagdown \quad \diagup \\ \circ \quad \circ \\ \diagup \quad \diagdown \\ \circ \end{array} + \begin{array}{c} \bullet \\ \diagdown \quad \diagup \\ \circ \quad \circ \\ \diagup \quad \diagdown \\ \bullet \end{array} - \begin{array}{c} \bullet \\ \diagdown \quad \diagup \\ \circ \quad \circ \\ \diagup \quad \diagdown \\ \bullet \end{array} = 0. \quad (15)$$

By foreshadowing that all contributions taken together yield 0, we have implied here that the symmetry factors are the same, no matter if we compose the diagrams only with interactions  $K$ , with elements of  $\frac{\partial \Gamma}{\partial \mathbf{v}}$  or a mixture of both, and that only their signs change. For order four, it is straight-forward to convince ourselves explicitly that this is true.

Indeed, the ring diagrams, equation (15), translate to

$$- \left( \frac{1}{4!} \frac{1}{2^4} \right) \cdot \left( \frac{4!}{4 \cdot 2} \cdot 2^4 \right) \cdot 2 \sum_{i \neq j \neq k \neq i} v_j J_{ij}^2 v_i^2 J_{ik}^2 v_k \quad (16)$$

$$- \left( \frac{1}{2 \cdot 2^2} \right) \cdot (2^2 \cdot 2) \sum_{i \neq j} \frac{\partial \Gamma}{\partial v_i} v_i^2 J_{ij}^2 v_j - \frac{1}{2} \cdot 2 \sum_i \frac{\partial \Gamma}{\partial v_i} v_i^2 \frac{\partial \Gamma}{\partial v_i} \quad (17)$$

$$= - \frac{1}{4} \sum_{i \neq j \neq k \neq i} J_{ij}^2 v_i^2 J_{ik}^2 + \frac{1}{2} \sum_{i \neq j} \sum_{k \neq i} v_k J_{ik}^2 v_i^2 J_{ij}^2 v_j - \frac{1}{4} \sum_i \sum_{k \neq i} v_k J_{ik}^2 v_i^2 \sum_{j \neq i} v_j J_{ij}^2 = 0,$$

where we indicate the origin of the prefactors of the terms in equation (16) and equation (17), which is coming about by the Feynman rules described in [9] and we which recall for this example :

- The ring diagrams composed of  $K$ s, in equation (16), contributes with a prefactor  $\frac{1}{4!2^4}$ , the  $4!$  coming from the Taylor expansion in small couplings, the  $\frac{1}{2^4}$  from the fact that each of them contributes with a factor  $\frac{1}{2}$ . We recall that to determine the symmetry factor of a diagram, we label its inner legs by indices and count the number of symmetry operations (permutation of vertices and flipping the legs of a vertex) that generate new combinations of labels, that is, new labeled diagrams. There are  $4!$  ways to permute the four interactions, but  $4 \cdot 2$  of them lead to the same labeled diagram because of the symmetry of the ring; one can start counting at every node and either go clockwise or counter-clockwise. Then, all  $2^4$  possible vertex flips generate new labeled diagrams, so that the symmetry factor is as

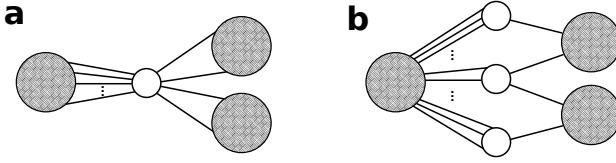


**Figure 1.** Sketch of (a) a cactus diagram and (b) an improper pseudo-cactus diagram.

indicated in the second bracket. While this is true of the ring diagrams without restrictions we here obtain an additional factor 2 because of the two possibilities to identify pairs of opposite nodes bearing the same index.

- In the first term of equation (17), we have the prefactor  $\frac{1}{2}$  because of the second order in  $K$  and  $\frac{1}{2^2}$  every one  $K$ 's comes with an  $\frac{1}{2}$  and the symmetry factor is  $2^2 \cdot 2$  because flipping either of the  $K$ 's or the  $\frac{\partial \Gamma}{\partial v}$ -vertex generates a new labeled diagram.
- In the second term of equation (17), we again have a prefactor  $\frac{1}{2}$  because of the double occurrence of a vertex, this time the one from  $\frac{\partial \Gamma}{\partial v}$  and the symmetry factor is 2 because we can flip one of them to generate a new labeled diagram (but flipping both brings back the original one).

The final contribution of all ring diagrams of order four therefore only contains the contributions with four pairwise unequal indices and two pairs of nodes with identical indices:

$$-\frac{1}{8} \sum_{\substack{i \neq j \neq k \neq l \neq i \\ i \neq k, j \neq l}} v_i K_{ij} v_j K_{jk} v_k K_{kl} v_l K_{li} + \frac{1}{8} \sum_{i \neq j} v_i^4 K_{ij}^4 v_j^4.$$

The reasoning for the “spectacles” diagram, as shown in equation (14) is analogous. The diagrams including  $\frac{\partial \Gamma}{\partial v_i}$  comes with the very same prefactors as the contributions before, only divided by 2 because they are no two nodes to choose from.‡ Correspondingly, also the spectacles diagram composed just of  $K$ s comes with a prefactor of  $\frac{1}{8}$  instead of  $\frac{1}{4}$  - indeed we have the same factor of  $\frac{1}{4!2^4}$  as for the ring diagram, 3 possibilities to pair vertices on either side and  $2^4$  vertex flips generating new diagrams. Therefore, we have confirmed that also this contribution is canceled.

*2.1.4. Cancellations in higher orders* We now proceed to higher orders, leveraging the ideas employed for the second-order terms. To do this, we introduce the notion of a counter diagram: it has the same form as a diagram in the diagrammatic expansion of  $W$ , but it contributes with the opposite sign. We will see that there are counter diagrams for two types of diagrams, defined by consisting of

‡ It might appear a bit odd at first sight that there is difference between the two cases because topologically the two nodes of order 2 play the same role as that of order 4. However, consider the origin of the prefactors: they come about by letting differential operators act on  $W_0$ . In case of the ring diagrams, this means: Two cumulants of order 1 each are generated by first letting the derivatives associated to one  $\frac{\partial \Gamma^K}{\partial v}$  vertex act on  $W_0$ . Then, letting the other  $\frac{\partial \Gamma^K}{\partial v}$  vertex act on these two cumulants there are always two ways of picking one of them. In contrast, for the four-point cumulant, one does not have this choice. In other words, when it comes to symmetry factors the two cumulants of order 2 are different than one cumulant of order 4.

- (i) multiple sub-diagrams connected only by a single node and at least one of them is connected to the node by exactly two lines. Generalizing this notion from the literature, we call these diagrams cactus diagrams (figure 1a)
- (ii) multiple sub-diagrams connected only by nodes joined by dotted lines and at least of the sub-diagrams is connected to the two nodes by exactly two lines (each of the two lines ending in a different node). Henceforth, we call collections of two-leg nodes with associated with identical indices (indicated by dotted lines) pseudo-nodes and, accordingly, the diagrams pseudo-cactus diagrams (figure 1b).

The notion of counter diagrams is similar to that of compensating diagrams of Vasiliev and Radzhabov, introduced in the study of the diagrammatics of the Ising model [21]. We discuss this point in a bit more detail in section §4 and leave a more thorough exploration of this link to future work.

Letting  $\frac{\partial}{\partial v_i}$  act on that part of  $\Gamma_{\text{int}}$  containing a second-order cumulant, this yields

$$\frac{\partial \Gamma^J}{\partial v_i} \left[ \left( \frac{\partial}{\partial j_i} - m_i \right)^2 - v_i \right] \supseteq - \text{diag} \left( \begin{array}{c} \partial_{j_i} \\ \text{---} \\ \text{---} \\ \partial_{j_i} \end{array} \right). \quad (18)$$

Labeling the diagram with derivatives with respect to  $j_i$ , we have taken into account that the contributions  $-m_i$  and  $-v_i$  on the left hand side just remove trivial contributions, in which the sub-diagram is attached to isolated cumulants of order one or two. The  $\partial_{j_i}$  operators, in turn, can either act on the same cumulant or on two different ones, corresponding to the points 1 and 2 above, respectively. For the fourth order, we have already shown that this leads to cancellation because the new diagrams contribute with the same prefactors. We convince ourselves that the same is true in the general case. As already argued in [9, sec. 2.4.1.], it is enough to compare the prefactors of the subdiagrams. Indeed, when considering the diagrams only constructed from  $K_{ij}$ , say, of order  $n$ , with  $k$  interactions in one sub-diagram and  $n - k$  interactions in the other part, we can determine its overall symmetry factor by first counting the ways one can distribute the interactions on the two subdiagrams: there are  $\binom{n}{k}$  to do so. This is combined with the overall prefactor of the diagram to yield  $\binom{n}{k} \frac{1}{n!} = \frac{1}{k!(n-k)!}$ , the same one we obtain from assembling the sub-diagrams and adding them afterwards. The only aspect that is different than in [9] is that we stick together the subdiagrams at two legs, instead of one. The resulting differences in the symmetry factors are the same, no matter if we construct the diagrams with  $\frac{\partial \Gamma^K}{\partial v}$  vertices or with  $K$ s.

We now address the question in which cases the existence of counter diagrams leads to a cancellation. In fact, this is always the case for the diagrams described in point 1 above, but not for the diagrams in point 2.

We will discuss this issue by considering ring diagrams - because they are the simplest examples and also the most relevant for applications. By treating all indices on the same footing (not taking into account any possibilities of identifications), the prefactor of a ring diagrams of order  $n$  is  $\frac{1}{n!} \frac{1}{2^n} \frac{n!}{2n} 2^n = \frac{1}{2n}$ . Indeed, every vertex flip generates a new labeled diagram, but not every permutation of vertices because one can start counting them at any node and label them clockwise or counter-clockwise.

We first study the ring diagram of sixth order in figure 2a. When one considers the two pairs of nodes connected by dotted lines as one node, it can be seen as three

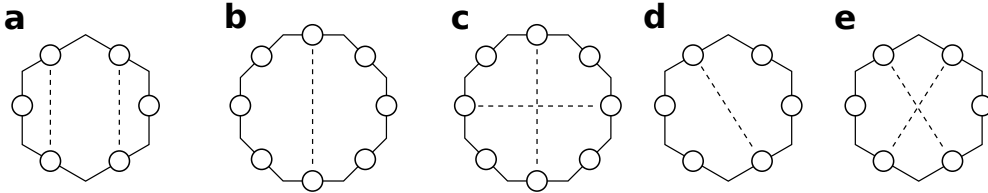


**Figure 2.** Ring diagrams with possible pairs of nodes with identical indices indicated by dotted lines.

concatenated rings of length 2, so a pseudo-cactus diagram. Complementing it with its counter diagrams, we can convince ourselves that it cancels (with the prefactors  $\frac{1}{4} - \frac{1}{2} + \frac{1}{4}$ ). We now proceed to the diagram of eighth order depicted in figure 2b, in which we identify the indices of one pair of nodes opposite in the ring. There are four of these pairs to choose from, so that the prefactor is  $\frac{1}{16} \cdot 4 = \frac{1}{4}$ . We can as well build this diagram with one of the half-rings replaced by a  $\frac{\partial \Gamma^K}{\partial v}$ -vertex, yielding the prefactor  $-\frac{1}{2}$  or both replaced, yielding  $\frac{1}{4}$ . This contribution therefore cancels. We next choose not only one pair of nodes to bear to same index, but two of them, the second pair “rotated” by 90 degrees with respect to the first one, as in figure 2c. We will call this a crossing identification (compare the notion of crossing partitions in the study of free probability theory [16]). We here have only 2 possibilities to pick these two pairs and therefore the prefactor for the diagram composed only of  $K$ 's is  $\frac{1}{16} \cdot 2 = \frac{1}{8}$ . In particular, the counter diagrams, however, keep their prefactors because we fix one pair of indices to cut the ring and replace the sub-diagrams by  $\frac{\partial \Gamma^K}{\partial v}$  and the second pair of indices is already fixed by this choice. Therefore, if there are multiple pairs of nodes with indices identified in such a way that one cannot represent the resulting diagram as a pseudo-cactus there is no guarantee that this contribution is canceled. This is due to the fact that in these cases, not for all pairs of nodes with identical indices, there are matching counter diagrams. In other words, the counter diagrams fail to cancel the original contributions because the diagram with the crossing identification has a different (higher) symmetry than the diagram with the single pair of nodes. This is analogous to the case of the contributions from the ring diagrams in fourth order in  $K$  with one or two pairs of nodes with identical indices.

We note for completeness, however, that there are also cases of diagrams with crossing identifications that do cancel, like in figure 2e. There, as well as in figure 2d, there are 3 possibilities to choose the respective pairs from. Because the symmetry of figure 2d is decisive for the prefactor of the counter diagrams, also the diagram with crossing identification gets canceled in this case - because the number of possible identifications of pairs is the same in both cases.

Either way, we have now seen that pseudo-cactus diagrams without crossing identifications, like that in figure 2a, get canceled. For proper cactus diagrams, these complications do not exist because one does not have to identify possible pseudo nodes, the cumulants are simply what they are.

Summarized, the following types of diagrams cancel:

- (i) Cactus diagrams
- (ii) Pseudo-cactus diagrams without crossing identifications

Before closing this section, we note that we did not characterize all diagrams contributing to  $\Gamma^K$ , but only those of the same type as those contributing to  $W$ .

However,  $\Gamma^K$  includes of course contributions with cumulants of orders higher than 2. Differentiating those with respect to  $m_i$  or  $v_i$  requires to take the derivative of the cumulant with respect to  $j_i$  and  $k_i$  to obtain the dependence on  $m_i$  and  $v_i$  via the inner derivatives. The latter is basically given by the Hessian of  $\Gamma_0^K$ , which for completeness we derive in section 5.1. These  $\Gamma^K$ -derivatives serve as vertices in the construction of higher orders - the lowest one being 6. However, in the application we will address in section 3.1, we do not need them because their contribution is sub-leading in the thermodynamic limit.

## 2.2. The Gaussian Legendre transform: $\Gamma^c$

In addition to the Legendre transforms on the one-point source fields  $\mathbf{j}$  and  $\mathbf{k}$ , one can also transform with respect to the two-point source field  $K$ , therefore fixing the covariances, which we denote as

$$\Gamma^c[\mathbf{m}, \mathbf{v}, c] := \sup_{\mathbf{j}, \mathbf{k}, K} \left[ \sum_i (m_i j_i + (v_i + m_i^2) k_i) + \frac{1}{2} \text{tr} (K (c + \mathbf{m} \mathbf{m}^T)) - W[\mathbf{j}, \mathbf{k}, K] \right].$$

We will call this the Gaussian Legendre transform because it depends on all cumulants present in a Gaussian theory. When applied to an actual Gaussian theory it is therefore what Vasiliev calls a complete Legendre transform [22, sec. 6.2.]. Its equations of state are

$$\frac{\partial \Gamma^c}{\partial m_i} = j_i + 2m_i k_i + \sum_{j(\neq i)} K_{ij} m_j$$

$$\frac{\partial \Gamma^c}{\partial v_i} = k_i$$

$$\frac{\partial \Gamma^c}{\partial c_{ij}} = K_{ij}.$$

*2.2.1. Derivation of a perturbation expansion for  $\Gamma^c$*  To derive the iteration equation for a diagrammatic expansion in this quantity, we proceed analogously to section 2.1.1 to obtain

$$\exp(-\Gamma_v^c[\mathbf{m}, \mathbf{v}]) = e^{-W_0[\mathbf{j}_0, \mathbf{k}_0]} \lim_{L \rightarrow \infty} \left( 1 + \frac{1}{L} A_c \left( \frac{\partial}{\partial \mathbf{j}} \right) \right)^L e^{W_0[\mathbf{j}_0, \mathbf{k}_0]}, \quad (19)$$

where

$$A_c \left( \frac{\partial}{\partial \mathbf{j}} \right) := \left( \frac{\partial \Gamma^c}{\partial \mathbf{m}} \right)^T \left( \frac{\partial}{\partial \mathbf{j}} - \mathbf{m} \right) \quad (20)$$

$$+ \left( \frac{\partial \Gamma^c}{\partial \mathbf{v}} \right)^T \left[ \left( \frac{\partial}{\partial \mathbf{j}} - \mathbf{m} \right)^2 - \mathbf{v} \right] \quad (21)$$

$$+ \frac{1}{2} \text{tr} \left( \frac{\partial \Gamma^c}{\partial c} \left[ \left( \frac{\partial}{\partial \mathbf{j}} - \mathbf{m} \right) \left( \frac{\partial}{\partial \mathbf{j}} - \mathbf{m} \right)^T - c \right] \right). \quad (22)$$

Note that because the interaction has the form of an off-diagonal two-point source field, which we have replaced by  $\frac{\partial \Gamma^c}{\partial c}$ ,  $H_V$  does not occur here anymore. The tricky part now is that for  $\Gamma^c$ , the expansion parameter is  $c$  instead of  $K$ . Therefore,

$\frac{\partial \Gamma^c}{\partial c}$  is of one order lower than  $\Gamma^c$ . Consequently, evaluating equation (19) at a fixed order  $n$  in  $c$  involves  $c$ -derivatives of the  $n$ -th order term also on the right-hand side - a priori. However, we will see that these terms are canceled for  $n > 2$  (compare also [11, sec. 5.1.4.]). In order to see this, we treat the order 2 separately. Here, it is straightforward to perform the additional Legendre transform with respect to  $K$  explicitly, obtaining  $\Gamma^c$  from  $\Gamma^K$ :

$$\begin{aligned} \Gamma^c[\mathbf{m}, \mathbf{v}, c] &= \sup_K \left[ \frac{1}{2} \text{tr} (K (c + \mathbf{m} \mathbf{m}^T)) + \Gamma^K[\mathbf{m}, \mathbf{v}, K] \right], \\ &= \sup_K \left[ \frac{1}{2} \sum_{i \neq j} K_{ij} (c_{ij} + m_i m_j) + \Gamma^K[\mathbf{m}, \mathbf{v}, K] \right] \end{aligned} \quad (23)$$

where

$$\Gamma^K[\mathbf{m}, \mathbf{v}, K] = \Gamma_0^K[\mathbf{m}, \mathbf{v}] - \frac{1}{2} \sum_{i \neq j} K_{ij} m_i m_j - \frac{1}{4} \sum_{i \neq j} K_{ij}^2 v_i v_j + \mathcal{O}(K^3).$$

Evaluating the condition on  $K$  given by the supremum by differentiating with respect to  $K_{ij}$ , we obtain

$$c_{ij} = K_{ij} v_i v_j.$$

Solving for  $K_{ij}$  and inserting into equation (23), we obtain§

$$\Gamma^c[\mathbf{m}, \mathbf{v}, c] = \Gamma_0^K[\mathbf{m}, \mathbf{v}] + \frac{1}{4} \sum_{i \neq j} \frac{c_{ij}^2}{v_i v_j} + \mathcal{O}(c^3). \quad (24)$$

Considering higher orders now, we obtain as our first estimate of  $\frac{\partial \Gamma^c}{\partial c}$  entering into equation (22)

$$\frac{\partial \Gamma^c}{\partial c_{ij}} = \frac{c_{ij}}{v_i v_j} + \mathcal{O}(c^2). \quad (25)$$

Now we can address the issue of what happens with the  $c$ -derivative of the terms of  $n$ -th order on the right-hand side of equation (19), evaluated at order  $n > 2$ : the contribution from  $\frac{\partial \Gamma^c}{\partial c}$  has to be combined with a term of order 1 to yield a  $n$ -th-order term, so either the  $-c$  in the definition of  $A_c$ , equation (22), or the derivative of the second-order contribution to  $\Gamma^c$  with respect to  $c$ . With equation (25), we see that both resulting terms are actually equal, up to the sign, and therefore cancel. For a more detailed discussion of this point, see [11, sec. 5.1.4.].

Therefore, from this point on, we can proceed largely analogous to the construction of the diagrammatic expansion of  $\Gamma^K$ , the only difference being that now, the newly generated vertices are not only coming from derivatives of the single-spin cumulants, represented by nodes, but also the covariances, which the edges represent now - slightly abusing diagrammatic notation, as in

$$\begin{array}{c} \diagup \\ i \quad j \\ \diagdown \end{array} = \frac{c_{ij}}{v_i v_j}, \quad (26)$$

§ This derivation demonstrates that [11, eq. (40)] is actually the correct second-order contribution to the free energy at fixed covariance and not just a consequence of a specific solution to the tensor equation [11, eq. (38)].

whereas nodes still represent cumulants of the uncoupled theory. For a detailed discussion of the contributions to this expansion coming about by the terms also present in the differential operator  $A_c$  without transform with respect to  $\mathbf{k}$ , equation (20) and equation (22), up to order four, we refer to [11, sec. 5.1.5. and 5.1.6.] and we will limit ourselves to studying the differences occurring due to the new part of  $A_c$ , equation (21), which starts contributing at fourth order.

*2.2.2. The fourth order of the Gaussian Legendre* In fourth order, equation (21) generates two contributions, largely analogous to equation (9). Note however, that here, the dependence on  $v_i$  is a different one than for  $\Gamma^K$  because it is contained not only through the single-spin contributions, but also in the interaction. However, differentiating the second-order correction in equation (24) with respect to  $v_i$ , we obtain

$$\frac{\partial}{\partial v_k} \frac{1}{4} \sum_{i \neq j} \frac{c_{ij}^2}{v_i v_j} = - \sum_{i(\neq k)} \frac{c_{ik}^2}{v_i v_k^2} = - \sum_{i(\neq k)} \left( \frac{c_{ik}}{v_i v_k} \right)^2 v_i = - \text{Diagram}, \quad (27)$$

so the analogous contribution to that of  $\Gamma^K$ . Consequently, it has the same effect on the spectacles diagram as for  $\Gamma^K$ : it gets canceled, as in equation (14).

Then, it generates a ring diagram with two pairs of indices identified, with the prefactor  $-\frac{1}{4}$ , when both halves of the ring come from  $\frac{\partial \Gamma^c}{\partial v_i}$ , and  $\frac{1}{2}$  when only one does. This contribution is combined with the other terms, generated by equation (22), therefore involving  $\frac{\partial \Gamma^c}{\partial c}$ .

The reasoning to determine the symmetry factors for the remaining terms is very similar to the contributions described before and it has been presented in [11, eq. (58) - (61)]. We therefore do not discuss it in detail here and simply state the result that by taking all terms together, we obtain

$$- \text{Diagram} + \frac{\partial \Gamma^K}{\partial c} \text{Diagram} - \frac{\partial \Gamma^K}{\partial c} \text{Diagram} \frac{\partial \Gamma^K}{\partial c} \quad (28)$$

$$+ \frac{\partial \Gamma^K}{\partial v} \text{Diagram} - \frac{\partial \Gamma^K}{\partial v} \text{Diagram} \frac{\partial \Gamma^K}{\partial v}, \quad (29)$$

where dotted lines denote pairs of nodes with indices that are explicitly unequal. This translates into

$$- \frac{1}{8} \sum_{i \neq j \neq k \neq l \neq i} K_{ik} v_k K_{kj} v_j K_{jl} v_l K_{li} v_i \quad (30)$$

$$+ \frac{1}{2} \sum_{i \neq j} \sum_{k, l(\neq i, j)} K_{ik} v_k K_{kj} v_j K_{jl} v_l K_{li} v_i - \frac{1}{4} \sum_{i \neq j} \sum_{k, l(\neq i, j)} K_{ik} v_k K_{kj} v_j K_{jl} v_l K_{li} v_i \quad (31)$$

$$+ \frac{1}{2} \sum_{i \neq j} \sum_{k(\neq i, j)} v_i K_{ik}^2 v_k^2 K_{jk}^2 v_j - \frac{1}{4} \sum_{i \neq j} \sum_{k(\neq i, j)} v_i K_{ik}^2 v_k^2 K_{jk}^2 v_j \quad (32)$$

$$= \frac{1}{8} \sum_{\substack{i \neq j \neq k \neq l \neq i, \\ i \neq k, j \neq l}} K_{ik} v_k K_{kj} v_j K_{jl} v_l K_{li} v_i + \frac{1}{4} \sum_{i \neq j} \sum_{k(\neq i, j)} v_i K_{ik}^2 v_k^2 K_{jk}^2 v_j + \frac{1}{8} \sum_{i \neq j} v_i v_i^4 K_{ij}^4 \quad (33)$$

which can be rewritten as

$$\frac{1}{8} \sum_{i \neq j \neq k \neq l \neq i} K_{ik} v_k K_{kj} v_j K_{jl} v_l K_{li} v_i = \frac{1}{8} \text{tr} \left( (Kv)^4 \right).$$

In other words: fixing also the (on-site) variance, in addition to the covariances, leads to a simplification because we do not have to differentiate between subsets of indices with different numbers of them identified. Indeed, without the additional part of the differential operator  $A_c$  in equation (21), we would only have the diagrams in equation (28), the latter two of which with the restriction that one pair of opposite nodes bears unequal indices. Only by the other two diagrams, this restriction is lifted because it adds exactly the complementary contributions. This is actually a general rule, as we will discuss in the next section.

*2.2.3. Ring diagrams in the Gaussian Legendre transform* We can generalize the insights gained for the fourth-order ring diagram to arbitrary order, which will allow us to resum this class of diagrams.

In [11], the sub-class of ring diagrams with indices that are pairwise unequal was characterized. If the index set is continuous (like, e.g., for simple liquids), this is sufficient for a straight-forward resummation. Otherwise it is not because the condition on all indices to be pairwise unequal prevents expressing this problem as a simple matrix equation. However, this is different if one includes an additional transform with respect to the variances. In this case one obtains additional contributions according to equation (21), which fixes this problem.

We will demonstrate that the prefactor of the ring diagram of order  $n$  is  $\frac{(-1)^n}{2^n}$  - and, in contrast to [11], the sum over the multiple indices it implies bears no further restriction than that directly neighbored nodes bear unequal indices. When constructing a ring diagram of order  $n$ , the following components are provided:

- concatenations of interactions, which we will call snake diagrams, of length  $k = 1, 2, \dots, n - 2$  with the condition that the outer indices are unequal, coming about from equation (22), with symmetry factor  $(-1)^{k+1}$
- snake diagrams of length  $2, \dots, n - 2$  with the condition that the outer indices are equal, coming about from part equation (21) of the operator  $A$ , with symmetry factor  $\frac{1}{2} (-1)^{k+1}$

The sign of both contribution derives from the respective ring diagrams the snakes come from: the first comes about by differentiating the the ring diagram of order  $k + 1$  with respect to the covariance, hence  $(-1)^{k+1}$ , the second comes from differentiating the ring diagram of order  $k$  (sign  $(-1)^k$ ) with respect to a variance. In the latter case, the dependence is of the form  $\frac{1}{v_i}$ , hence the prefactor of this snake diagram is  $(-1)^{k+1}$  as well. The difference in the symmetry factor comes about by the fact that in the first case, one differentiates with respect to a two-point quantity (the covariance), whereas in the second case, one differentiates with respect to a one-point quantity (the variance). Inserted into equation (22) and equation (21), respectively, one observes that both contributions act in exactly the same way on the unperturbed cumulants, only with opposite - or, rather, complementary - restrictions on the outer indices, because equation (22) has an additional factor  $\frac{1}{2}$  compared to equation (21). Because of the many ways one can partition  $n$  to subdivide the ring into snakes|| it

|| For being precise, one has to add: discarding the option to include snake diagrams of order  $n - 1$ , according to the rules derived in [11] and recapitulated in section 2.2.1.

is far from obvious that the resulting prefactor is indeed  $\frac{(-1)^n}{2^n}$ . However, this result is proven in [11, sec. 8 and Appendix], without alluding to the fact that indices are pairwise unequal, actually not assuming anything about the summation, but simply assuming that the sums are performed for the right index set. With the additional contribution of two-point interactions with identical interactions, we have lifted the need to distinguish these cases because no matter how the ring is partitioned, there are no additional restrictions imposed on the indices.

Therefore, the argument of [11] for the resummation of ring diagrams now literally carries over, only without the restriction to pairwise unequal indices. This has to be so because for a Gaussian theory, one knows that the entropy equals

$$S - \frac{N}{2} \ln(2\pi e) = \frac{1}{2} \ln(c) = \frac{1}{2} \sum_i \ln(V_i) + \frac{1}{2} \text{tr} \left( \sum_{n=2}^{\infty} \frac{(-1)^{n+1}}{n} \left( \frac{c_{\neq}}{\sqrt{V}\sqrt{V}} \right)^n \right) \quad (34)$$

$$\text{where} \left( \frac{c_{\neq}}{\sqrt{V}\sqrt{V}} \right)^n = \sum_{i_1 \neq i_2 \neq \dots \neq i_{n-1} \neq i_1} \frac{c_{i_1 i_2}}{V_{i_1}} \frac{c_{i_2 i_3}}{V_{i_2}} \dots \frac{c_{i_{n-1} i_1}}{V_{i_{n-1}}} \quad (35)$$

In the sum into which the matrix power translates, the only restriction is upon neighbored indices. This corresponds to the resummation of all ring diagrams without the indices having to be pairwise unequal.

### 3. Applications

#### 3.1. $p$ -spins coupled by rotationally invariant matrices

We here consider the example from Maillard et al. [12] to study message-passing algorithms. They consider an interacting part of the Hamiltonian of the form

$$H_V = -\frac{1}{2} \sum_{1 \leq i \neq j \leq N} x_i J_{ij} x_j,$$

where  $J$  is a symmetric rotationally invariant matrix (their model S) and the  $x_i$  are  $p$ -spins (the type of  $x_i$  does not matter for us, but choosing it as a  $p$ -spin has the merit that it allows to derive the exact expression of the free energy in the thermodynamic limit by other means than a small-coupling expansion. There is therefore a ground truth to compare with.). We have excluded diagonal terms, unlike Maillard et al. do, however, we can absorb it into the two-point source-field, so both is fine. Extending the work of Plefka and Georges/Yedidia [3, 18] to the Legendre transform at fixed mean and variance, Maillard et al. set up a small-coupling expansion. It is, however, not diagrammatic; the diagrams they are drawing are depictions of the terms they have derived by other means. In addition, they build on a result from random-matrix theory by Guionnet et al. [4] to show that out of these contributions only those remain that they call simple cycles and cacti, all other vanish in the thermodynamic limit of  $N \rightarrow \infty$ . Their simple cycle (see their sec. 5.2) corresponds to a ring diagram with all indices pairwise unequal in our terminology. Cactus diagrams in their terminology comprise what we call cactus and pseudo-cactus diagrams with all sub-diagrams being simple cycles (because the other ones are irrelevant in the thermodynamic limit). They convince themselves by explicit computation that up to fourth order, the cactus diagrams are canceled in the small-coupling expansion. They therefore conjecture the

free energy to be (their eq. (25) , note that they scale their free energy with  $\frac{1}{N}$ , which we do not)

$$\Gamma^K = \Gamma_0^K + \frac{1}{2} \sum_{i \neq j} J_{ij} m_i m_j + \sum_{p=2}^{\infty} \frac{1}{2^p} \sum_{\substack{i_1, \dots, i_p \\ \text{pairwisely distinct}}} v_{i_1} J_{i_1 i_2} v_{i_2} J_{i_2 i_3} \dots J_{i_{p-1} i_p} + o_N(1), \quad (36)$$

assuming that cactus diagrams cancel in all orders. Still the formalism of Georges and Yedidia [3] “can not (somehow disappointingly) give an analytic result for an arbitrary perturbation order  $n$ ”, as Maillard et al. write.

With our insights from section 2.1.4, we now fill this gap and complete their proof, rendering their conjecture into a theorem. The only qualm that one could have is that, as discussed in section 2.1.4, we actually do not cancel all pseudo-cactus diagrams. However, the ones that are not canceled are the ones with the crossing identities and they are therefore of the type that Maillard et al. call strongly irreducible - and therefore vanish in the thermodynamic limit. Indeed, because of the very structure of our diagrammatics, we construct a counter diagram with matching prefactor in all of the cases, which are “dangerous” in the sense of Maillard et al., that is, in the case of sticking together together simple cycles.

### 3.2. The Gaussian Legendre transform as a (maximum) entropy

An important application of our results on the joint Legendre transform with respect to  $\mathbf{j}$ ,  $\mathbf{k}$  and  $K$  is to estimate the maximum value for the entropy given the first two moments of some data set. The corresponding probability distribution is indeed given by [7]

$$P_{\text{MaxEnt}}(\mathbf{n}) = \frac{1}{\mathcal{Z}(\mathbf{j}, \mathbf{k}, K)} e^{\sum_i (j_i n_i + k_i n_i^2) + \sum_{i \neq j} K_{ij} n_i n_j}$$

and the corresponding entropy therefore is

$$S = \left\langle - \sum_i (j_i n_i + k_i n_i^2) - \sum_{i \neq j} K_{ij} n_i n_j \right\rangle_{\mathbf{n}} + \ln(\mathcal{Z}(\mathbf{j}, \mathbf{k}, K)).$$

We can express that fact that the source fields are chosen such that the first two moments of the model fit the measured ones by adding a supremum, yielding

$$S = \sup_{\mathbf{j}, \mathbf{k}, K} \left[ \left\langle - \sum_i (j_i n_i + k_i n_i^2) - \sum_{i \neq j} K_{ij} n_i n_j \right\rangle_{\mathbf{n}} + \ln(\mathcal{Z}(\mathbf{j}, \mathbf{k}, K)) \right] = -\Gamma^c[\mathbf{m}, \mathbf{v}, c]. \quad (37)$$

We note in passing that this is also consistent with the thermodynamic definition of the (Helmholtz) free energy as the Legendre transform of the entropy with respect to the energy.

With the relation equation (37) at hand, we can use the results from section 2.2, to estimate entropies from empirical probability distributions. This is particularly useful when the data is poorly sampled and a direct estimate of the entropy is therefore prone to biases [15]. In particular section 2.2.3 then enables a stable estimate, without being too restrictive with respect to the form of the underlying probability distribution. In particular, it avoids assuming a Gaussian shape, but allows to exactly take into account the single-spin contributions to the entropy.

We can also imagine to not only fix the first two, but the whole single-spin probability distribution or all of its cumulants (which is equivalent given that all

cumulants exist). This would add another term to equation (20) for every additional condition.

For every finite order, of course, only a finite number of this terms contribute - in particular, the term in the differential operator  $A_c$  that comes about by fixing the  $n$ -th-order cumulant is of order  $n$  in the covariance (coming from the diagram with just two cumulants, connected by  $n$  interactions). Therefore the lowest-order correction to the free energy occurring because the variance is fixed, equation (21), is of order four. In any case, if one only considers diagrams of the ring type, the additional contributions to  $A_c$  are insubstantial because they generate diagrams of different topologies by construction. While the resummation of rings diagrams is usually an ad-hoc approach, there are cases in which it can be justified: if the covariances obey the mean-field scaling  $1/N$  with  $N$  the number of spins for example, the ring diagrams are the dominating ones for  $N \rightarrow \infty$ .

### 3.3. Ising model

The Ising model is special, because due to its binary character, one source field fixes all single-unit moments. This means that Legendre transforms of order higher than one are not well-defined for all arguments [6]. However, there is no problem if we evaluate only at the values given by the Ising model, that is

$$\begin{aligned} \langle n^{2k+1} \rangle &= m \\ \langle n^{2k} \rangle &= 1. \end{aligned}$$

*3.3.1. Fourth-order small-coupling expansion* It is not only possible, but also useful to formally define higher-order Legendre transforms because, as we will see, it simplifies the diagrammatics and explains puzzles that would remain unresolved if only the first transform were considered.

Actually, the first contributions to  $\Gamma^K$  in addition to that of the first Legendre transform, coming about from equation (9), are those discussed in section 2.1.3. They contribute to the fourth order, which in total reads

$$- \text{[spectacles diagram]} + \text{[ring diagram]} - \text{[diamond diagram]} - \text{[counter diagram]}, \quad (38)$$

because the spectacles diagram cancels, as in equation (14). This reproduces the result from [9] obtained from the first Legendre transform. There, the argument of the Legendre transform is just  $\mathbf{m}$ , necessitating inner derivatives when differentiating the second-order contribution to the free energy (the TAP term) to obtain  $\frac{\partial \Gamma^K}{\partial \mathbf{m}}$ , which leads to equation (48) in [9]. It contains the spectacles diagram and the corresponding terms with  $\frac{\partial \Gamma^K}{\partial \mathbf{m}}$ -derivatives, which taken together, with the cumulants of the Ising model inserted, generates the same expression as the counter diagram for the ring. This appeared quite mysterious in [9] - however, extending the Legendre transform to one involving the second-order source term gives now a much more natural and shorter derivation. A similar simplification of the Ising diagrammatics was already presented in [20–22, sec. 6.3.4.], however, featuring a quite technical derivation without link to Legendre transforms with respect to higher-order source fields.

*3.3.2. The ring resummation in the Ising model* The fact that for the Ising model Legendre transforms with respect to arbitrarily many source fields are identical to the first Legendre transform justifies the resummation of the ring diagrams expressed by matrix products for the Ising model as performed in [2, 19]. In particular, with this results, we can explain an observation of Cocco and Monasson [2, appendix B]. They note that a diagram depicting a term in their small-correlation expansion (the middle one in the second column of their figure 26) contributes with the same prefactor to the entropy as the corresponding term to what they call the mean-field approximation of the entropy, our equation (34). The reason for this is not obvious in their framework (which is not diagrammatic, but that from [19], the diagrams are just a depiction of terms derived by other means).

With our analysis, however, it is now apparent that this is neither a coincidence nor special to the fourth order - rather, it is a consequence of the fact that for the Ising model, equation (34) is the exact resummation of all ring diagrams, including summations over pairwise unequal indices (what is called loops in [2] and simple cycles in [12]) but also those with repeated indices.

#### 4. Discussion

In this manuscript, we have derived an extension of the diagrammatic framework developed in [9, 11] to encompass free energies as a function of the variances of a stochastic variable. We have demonstrated that this leads to diagrammatic rules harmoniously adding to those developed so far, which enable us to understand diverse perturbative expansions derived by other means. In particular, it allowed us to complete the proof of a result on a system characterized by a rotationally invariant matrix, which so far has only been conjectured [12], and to derive, on a theoretically grounded way, a practical approximation for the entropy of a complex system of which only a limited amount of statistics is available [10]. So while the present manuscript, as we believe, is a valid contribution because it relates known results to each other, thereby allows to better understand them and simplifies their derivation, we arguably have not derived any result that has not been already intuited or could have been guessed by “common sense”. However, because our diagrammatic framework indeed allows for comparatively simple and compact derivations of approximations, we believe that it will allow to tackle several timely problems that have been hard to treat because of technical difficulties so far and that we briefly discuss in the following.

The reason for which the free energy has been studied in [12] is that it allows the derivation of message-passing algorithms, an efficient way to compute the statistics of a system. Besides providing a way to solve many problems in data science, it is also at the core of their theoretical study [23]. In a follow-up work to [12] for example, Maillard et al. consider the problems of matrix factorization: finding the matrices  $F$  and  $X$  from the observation of a matrix  $Y$  obeying some law

$$Y \sim P(Y|FX).$$

In what is known as the Bayesian optimal setting, that is, the probability distribution  $P$  is known, as well as the prior distributions of  $F$  and  $X$ , this problem amounts to computing the joint probability distribution of  $Y$ ,  $F$  and  $X$ , which requires to compute the corresponding partition function - or, equivalently, the free energy. For most cases, it is infeasible to achieve this exactly. It is therefore a matter of ongoing research to find

good approximations for the free energy - and therefore for the corresponding message-passage algorithms - for the problem of matrix factorization and the related problem of matrix denoising [8, 13, and references therein]. This is particularly true for the the extensive-rank case, in which  $F$  and  $X$  have a rank in the same order as their size, which is treated in [13] by means of the Georges/Yedidia high-temperature expansion [3]. However, similar as in [12], an exhaustive exploration of this perturbative inroad to the problem is prevented by the technical limits of the Georges/Yedidia expansion. It is therefore a promising venue for future research to apply our diagrammatic framework to this problem and related questions.

Applying our approach as a tool to compute entropies of undersampled systems, its extension to higher-order interactions is a natural step to do, which promises to have multiple applications [1]. Formally treating them in our framework is straight-forward, however, we expect it to be challenging to derive useful approximations for them going beyond the lowest order in perturbation theory, in particular in case that Legendre transforms are performed with respect to the additional interactions. Here, approximations adapted to the concrete applications at hand could become necessary.

On the technical side, we note that our counter diagrams seem closely related to what Vasiliev and Radzhabov call compensating diagrams in their diagrammatics of the first Legendre transform for the Ising model [21, 22, sec. 6.3.4.]. Their analysis, however, is not restricted to sub-diagrams attached to the rest by two legs, as ours is (because counter diagrams come from differentiating  $\Gamma^K$  with respect to the two-point cumulant  $v_i$ ). Also, their derivation is very different from ours, in particular they do not refer to any Legendre transform of order higher than 1. Nonetheless, we reckon that their result could be obtained in a more straight-forward way by formally defining the complete Legendre form, that is, with respect to all source fields of arbitrary order, as indicated in section 3.3. This is another topic for future research.

## Acknowledgments

We thank Laura Foini and Claudia Merger for very helpful discussions.

We acknowledge funding by ANR-21-CE37-0024 NatNetNoise. This work has been done within the framework of the PostGenAI@Paris project and it has benefitted from financial support by the Agence Nationale de la Recherche (ANR) with the reference ANR-23-IACL-0007. Our lab is part of the DIM C-BRAINS, funded by the Conseil Régional d'Ile-de-France.

## 5. Appendix

### 5.1. General treatment of $\mathbf{m}$ - and $\mathbf{v}$ -dependence of unperturbed cumulants

In this section, we will derive the Hessian of  $\Gamma_0^K$ . We will omit the index  $i$  in the following. We have

$$\begin{aligned}
1 &= \frac{\partial m}{\partial m} &= \frac{\partial j}{\partial m} \frac{\partial^2 W}{\partial j^2} + \frac{\partial k}{\partial m} \frac{\partial^2 W}{\partial k \partial j} &= \frac{\partial}{\partial m} \left( \frac{\partial \Gamma}{\partial m} - 2m \frac{\partial \Gamma}{\partial v} \right) \frac{\partial^2 W}{\partial j^2} + \frac{\partial^2 \Gamma}{\partial v \partial m} \frac{\partial^2 W}{\partial k \partial j} \\
& &= \left( \frac{\partial^2 \Gamma}{\partial m^2} - 2 \frac{\partial \Gamma}{\partial v} - 2m \frac{\partial^2 \Gamma}{\partial m \partial v} \right) \frac{\partial^2 W}{\partial j^2} + \frac{\partial^2 \Gamma}{\partial v \partial m} \frac{\partial}{\partial j} \left( \frac{\partial^2 W}{\partial j^2} + \left( \frac{\partial W}{\partial j} \right)^2 \right) \\
& &= \left( \frac{\partial^2 \Gamma}{\partial m^2} - 2 \frac{\partial \Gamma}{\partial v} \right) \frac{\partial^2 W}{\partial j^2} + \frac{\partial^2 \Gamma}{\partial v \partial m} \frac{\partial^3 W}{\partial j^3}
\end{aligned}$$

$$\begin{aligned}
& \underbrace{-2m \frac{\partial^2 \Gamma}{\partial m \partial v} \frac{\partial^2 W}{\partial j^2} + 2 \frac{\partial^2 \Gamma}{\partial v \partial m} \frac{\partial W}{\partial j} \frac{\partial^2 W}{\partial j^2}}_{\frac{\partial W}{\partial j} = m_0} \\
0 = \frac{\partial m}{\partial v} &= \frac{\partial j}{\partial v} \frac{\partial^2 W}{\partial j^2} + \frac{\partial k}{\partial v} \frac{\partial^2 W}{\partial k \partial j} = \frac{\partial}{\partial v} \left( \frac{\partial \Gamma}{\partial m} - 2m \frac{\partial \Gamma}{\partial v} \right) \frac{\partial^2 W}{\partial j^2} + \frac{\partial^2 \Gamma}{\partial v^2} \frac{\partial^2 W}{\partial k \partial j} \\
&= \left( \frac{\partial^2 \Gamma}{\partial m \partial v} - 2m \frac{\partial^2 \Gamma}{\partial v^2} \right) \frac{\partial^2 W}{\partial j^2} + \frac{\partial^2 \Gamma}{\partial v^2} \frac{\partial}{\partial j} \left( \frac{\partial^2 W}{\partial j^2} + \left( \frac{\partial W}{\partial j} \right)^2 \right) \\
&= \frac{\partial^2 \Gamma}{\partial m \partial v} \frac{\partial^2 W}{\partial j^2} + \frac{\partial^2 \Gamma}{\partial v^2} \frac{\partial^3 W}{\partial j^3} \\
&\quad \underbrace{-2m \frac{\partial^2 \Gamma}{\partial v^2} \frac{\partial^2 W}{\partial j^2} + 2 \frac{\partial^2 \Gamma}{\partial v^2} \frac{\partial^2 W}{\partial j^2} \frac{\partial W}{\partial j}}_{\frac{\partial W}{\partial j} = m_0} \\
0 = \frac{\partial v}{\partial m} &= \frac{\partial j}{\partial m} \frac{\partial}{\partial j} \frac{\partial^2 W}{\partial j^2} + \frac{\partial k}{\partial m} \frac{\partial}{\partial k} \frac{\partial^2 W}{\partial j^2} = \frac{\partial}{\partial m} \left( \frac{\partial \Gamma}{\partial m} - 2m \frac{\partial \Gamma}{\partial v} \right) \frac{\partial^3 W}{\partial j^3} + \frac{\partial^2 \Gamma}{\partial m \partial v} \frac{\partial^2}{\partial j^2} \left( \frac{\partial^2 W}{\partial j^2} + \left( \frac{\partial W}{\partial j} \right)^2 \right) \\
&= \left( \frac{\partial^2 \Gamma}{\partial m^2} - 2 \frac{\partial \Gamma}{\partial v} \right) \frac{\partial^3 W}{\partial j^3} + \frac{\partial^2 \Gamma}{\partial m \partial v} \left( \frac{\partial^4 W}{\partial j^4} + 2 \left( \frac{\partial^2 W}{\partial j^2} \right)^2 \right) \\
&\quad \underbrace{-2m \frac{\partial^2 \Gamma}{\partial v \partial m} \frac{\partial^3 W}{\partial j^3} + \frac{\partial^2 \Gamma}{\partial m \partial v} 2 \frac{\partial W}{\partial j} \frac{\partial^3 W}{\partial j^3}}_{\frac{\partial W}{\partial j} = m_0} \\
1 = \frac{\partial v}{\partial m} &= \frac{\partial j}{\partial v} \frac{\partial}{\partial j} \frac{\partial^2 W}{\partial j^2} + \frac{\partial k}{\partial v} \frac{\partial}{\partial k} \frac{\partial^2 W}{\partial j^2} = \frac{\partial}{\partial v} \left( \frac{\partial \Gamma}{\partial m} - 2m \frac{\partial \Gamma}{\partial v} \right) \frac{\partial^3 W}{\partial j^3} + \frac{\partial^2 \Gamma}{\partial v^2} \frac{\partial^2}{\partial j^2} \left( \frac{\partial^2 W}{\partial j^2} + \left( \frac{\partial W}{\partial j} \right)^2 \right) \\
&= \frac{\partial^2 \Gamma}{\partial m \partial v} \frac{\partial^3 W}{\partial j^3} + \frac{\partial^2 \Gamma}{\partial v^2} \left( \frac{\partial^4 W}{\partial j^4} + 2 \left( \frac{\partial^2 W}{\partial j^2} \right)^2 \right) \\
&\quad \underbrace{-2m \frac{\partial^2 \Gamma}{\partial v^2} \frac{\partial^3 W}{\partial j^3} + \frac{\partial^2 \Gamma}{\partial v^2} 2 \frac{\partial W}{\partial j} \frac{\partial^2 W}{\partial j^2}}_{\frac{\partial W}{\partial j} = m_0}
\end{aligned}$$

In matrix form this reads

$$\begin{pmatrix} 1 & 0 \\ 0 & 1 \end{pmatrix} = \begin{pmatrix} \frac{\partial^2 \Gamma}{\partial m^2} - 2 \frac{\partial \Gamma}{\partial v} & \frac{\partial^2 \Gamma}{\partial m \partial v} \\ \frac{\partial^2 \Gamma}{\partial m \partial v} & \frac{\partial^2 \Gamma}{\partial v^2} \end{pmatrix} \begin{pmatrix} \frac{\partial^2 W}{\partial j^2} & \frac{\partial^3 W}{\partial j^3} \\ \frac{\partial^3 W}{\partial j^3} & \left( \frac{\partial^4 W}{\partial j^4} + 2 \left( \frac{\partial^2 W}{\partial j^2} \right)^2 \right) \end{pmatrix}.$$

From this result, we then obtain the desired inner derivatives as

$$\begin{aligned}
\frac{\partial j}{\partial m} &= \frac{\partial^2 \Gamma}{\partial m^2} - 2 \frac{\partial \Gamma}{\partial v} - 2m \frac{\partial^2 \Gamma}{\partial m \partial v} \\
\frac{\partial k}{\partial m} &= \frac{\partial^2 \Gamma}{\partial m \partial v} \\
\frac{\partial j}{\partial v} &= \frac{\partial^2 \Gamma}{\partial m \partial v} - 2m \frac{\partial^2 \Gamma}{\partial v^2} \\
\frac{\partial k}{\partial v} &= \frac{\partial^2 \Gamma}{\partial v^2},
\end{aligned}$$

that we would need to evaluate the additional diagrams coming about by  $\frac{\partial \Gamma^K}{\partial \mathbf{m}}$  and  $\frac{\partial \Gamma^K}{\partial \mathbf{v}}$  vertices containing cumulants of order higher than 2, which, however, we have not discussed in detail in this manuscript.

## References

- [1] Federico Battiston, Giulia Cencetti, Iacopo Iacopini, Vito Latora, Maxime Lucas, Alice Patania, Jean-Gabriel Young, and Giovanni Petri. Networks beyond pairwise interactions: Structure and dynamics. *Physics Reports*, 874:1–92, 2020. Networks beyond pairwise interactions: Structure and dynamics.
- [2] S. Cocco and R. Monasson. Adaptive cluster expansion for the inverse ising problem: Convergence, algorithm and tests. *Journal of Statistical Physics*, 147:252 – 314, 2012.
- [3] Antoine Georges and Jonathan S Yedidia. How to expand around mean-field theory using high-temperature expansions. *Journal of Physics A: Mathematical and General*, 24(9):2173, 1991.
- [4] A. Guionnet and M. Maïda. A fourier view on the r-transform and related asymptotics of spherical integrals. *Journal of Functional Analysis*, 222(2):435–490, 2005.
- [5] Jean-Pierre Hansen and Ian Ranald McDonald. *Theory of simple liquids: with applications to soft matter*. Academic press, 2013.
- [6] Hugo Jacquin and A. Rançon. Resummed mean-field inference for strongly coupled data. *Phys. Rev. E*, 94:042118, Oct 2016.
- [7] Edwin T Jaynes. *Probability theory: The logic of science*. Cambridge university press, 2003.
- [8] Yoshiyuki Kabashima, Florent Krzakala, Marc Mézard, Ayaka Sakata, and Lenka Zdeborová. Phase transitions and sample complexity in bayes-optimal matrix factorization. *IEEE Transactions on Information Theory*, 62(7):4228–4265, 2016.
- [9] Tobias Kühn and Moritz Helias. Expansion of the effective action around non-gaussian theories. *Journal of Physics A: Mathematical and Theoretical*, 51(37):375004, aug 2018.
- [10] Tobias Kühn, Gabriel Mahuas, and Ulisse Ferrari. Diagrammatic expansion for the mutual-information rate in the realm of limited statistics, in prep. 2025.
- [11] Tobias Kühn and Frédéric van Wijland. Diagrammatics for the inverse problem in spin systems and simple liquids. *Journal of Physics A: Mathematical and Theoretical*, 56(11):115001, feb 2023.
- [12] Antoine Maillard, Laura Foini, Alejandro Lage Castellanos, Florent Krzakala, Marc Mézard, and Lenka Zdeborová. High-temperature expansions and message passing algorithms. *Journal of Statistical Mechanics: Theory and Experiment*, 2019(11):113301, nov 2019.
- [13] Antoine Maillard, Florent Krzakala, Marc Mézard, and Lenka Zdeborová. Perturbative construction of mean-field equations in extensive-rank matrix factorization and denoising. *Journal of Statistical Mechanics: Theory and Experiment*, 2022(8):083301, aug 2022.

- [14] K Nakanishi and H Takayama. Mean-field theory for a spin-glass model of neural networks: Tap free energy and the paramagnetic to spin-glass transition. 30:8085–8094, 1997.
- [15] Liam Paninski. Estimation of entropy and mutual information. *Neural Computation*, 15(6):1191–1253, 06 2003.
- [16] Silvia Pappalardi, Laura Foini, and Jorge Kurchan. Eigenstate thermalization hypothesis and free probability. *Phys. Rev. Lett.*, 129:170603, Oct 2022.
- [17] G Parisi and M Potters. Mean-field equations for spin models with orthogonal interaction matrices. *Journal of Physics A: Mathematical and General*, 28(18):5267, sep 1995.
- [18] Timm Plefka. Convergence condition of the tap equation for the infinite-ranged ising spin glass model. *Journal of Physics A: Mathematical and general*, 15(6):1971, 1982.
- [19] Vitor Sessak and Rémi Monasson. Small-correlation expansions for the inverse ising problem. *Journal of Physics A: Mathematical and Theoretical*, 42(5):055001, 2009.
- [20] A. N. Vasiliev and R. A. Radzhabov. Legendre transforms in the ising model. *Theoretical and Mathematical Physics*, 21(1):963–970, 1974.
- [21] A. N. Vasiliev and R. A. Radzhabov. Analysis of the nonstar graphs of the legendre transform in the ising model. *Theoretical and Mathematical Physics*, 23(3):575–579, Jun 1975.
- [22] Aleksandr Nikolaevich Vasiliev. *Functional methods in quantum field theory and statistical physics*. Routledge, 2019.
- [23] Lenka Zdeborová and Florent Krzakala and. Statistical physics of inference: thresholds and algorithms. *Advances in Physics*, 65(5):453–552, 2016.
- [24] Jean Zinn-Justin. *Quantum field theory and critical phenomena*. Clarendon Press, Oxford, 1996.